

## X-ray diffraction of epitaxial films with arbitrarily correlated dislocations: Monte Carlo calculation and experiment

Vladimir M. Kaganer, Oliver Brandt, and Henning Riechert

*Paul-Drude-Institut für Festkörperelektronik, Hausvogteiplatz 5-7, 10117 Berlin, Germany*

Karl K. Sabelfeld

*Institute of Computational Mathematics and Mathematical Geophysics, Russian Academy of Sciences, Lavrentiev Prosp. 6, 630090 Novosibirsk, Russia*

(Received 13 July 2009; published 31 July 2009)

We present a Monte Carlo technique to calculate the x-ray diffraction profiles from films with arbitrarily correlated dislocation distributions. Both spatial integration and the integration over several dislocation ensembles are performed simultaneously. We explicitly consider the coexistence of misfit and threading dislocation ensembles with arbitrary correlations. Using these techniques, we are able to quantitatively reproduce the experimental lineshapes for both thin (less than 100 nm) and thick (more than 1000 nm) GaN epitaxial films on SiC. Our calculations explain the ubiquitous lineshape observed for thin, highly mismatched films, with a central coherent peak accompanied by exponentially decaying diffuse scattering.

DOI: [10.1103/PhysRevB.80.033306](https://doi.org/10.1103/PhysRevB.80.033306)

PACS number(s): 61.05.cp, 68.35.-p, 61.72.Dd, 61.72.Lk

The lattice mismatch between an epitaxial film and the substrate gives rise to elastic strain in the film. When the film thickness exceeds a critical value, the strain energy is relaxed by the creation of two types of dislocations, misfit dislocations at the film-substrate interface, and threading dislocations spanning the surface and the interface. The elastic energy is further relaxed by the development of correlations in the dislocation positions. The correlations are qualitatively different for misfit and threading dislocation ensembles.

The elastic energy of threading dislocations, similarly to the case of dislocations in bulk crystals,<sup>1</sup> is reduced by screening of the dislocation strain fields by surrounding dislocations. The effect of screening on the x-ray diffraction peak profiles from relaxed epitaxial films with threading dislocations has been studied both theoretically and experimentally.<sup>2-4</sup> On the other hand, misfit dislocations tend to arrange periodically, to reduce their elastic energy. Theoretical description of the x-ray diffraction from partially ordered misfit dislocations has been proposed<sup>5</sup> only in one limiting case, when the mean distance between dislocations is much smaller than the correlation length which, in turn, is much smaller than the film thickness. The correlations of either misfit or threading dislocations reduce the half width of the diffraction peaks. For large dislocation densities, the diffraction peaks possess a Gaussian shape at the center passing into a power-law asymptotic.

A quite different diffraction lineshape has been observed for thin (<100 nm) epitaxial films with a lattice mismatch of several percent. The x-ray diffraction experiments on a wide variety of materials, such as metals,<sup>6-10</sup> semiconductors,<sup>11-14</sup> oxides,<sup>15</sup> and ferroelectrics<sup>16,17</sup> report diffraction profiles consisting of a narrow central peak accompanied by a broad diffuse background. Different authors<sup>6-17</sup> finally agreed that misfit dislocations are the source of the two-component profiles. Barabash *et al.*<sup>18</sup> proposed a quantitative treatment of the peaks. They noted that the Debye-Waller factor for misfit dislocations in epitaxial films is not zero, in contrast to the case of dislocations in

bulk crystals,<sup>19</sup> and the coherent peak persists. However, a detailed calculation of the coherent intensity for uncorrelated misfit dislocations (see Fig. 5 in Ref. 5) shows that the coherent intensity decreases by two orders of magnitude, compared to a dislocation-free film, for the film thickness equal to the mean distance between dislocations. The coherent intensity decreases exponentially with further increase in the film thickness. This conclusion is confirmed by the calculations below shown by the green (thick) line in Fig. 1(b): for uncorrelated dislocations with the mean distance between dislocations two times smaller than the film thickness, the transverse peak already assumes a Gaussian shape, and a coherent peak is absent. The calculations below show that sufficiently strong correlations in the dislocation positions are required to prevent the coherent peak.

In this Brief Report, we propose a Monte Carlo method to calculate the x-ray diffraction of films with arbitrarily correlated lattice defects. Spatial integration and the average over defect statistics are performed simultaneously. Recently, Holy *et al.*<sup>20</sup> employed our initial idea of the Monte Carlo calculation of the diffraction peaks. They generated just one set of threading dislocations on random and performed the spatial integration by the standard quadratures. Since strongly oscillating functions make a numerical integration very difficult, they simplified the spatial integrals using the stationary-point approximation. In the Brief Report, in contrast to Ref. 20, we take into account the correlations in the dislocation positions, perform a statistical average over the dislocation ensemble, and perform the spatial integration also by the Monte Carlo method.

We consider misfit and threading dislocations in relaxed epitaxial films on an equal footing and primarily concentrate on moderate misfits (a few percent) and film thicknesses of several tens of nanometers, somewhat larger than the mean distance between dislocations. Relaxation of these films gives rise to edge (Lomer type) misfit dislocations that are able to glide along the interface and may order to reduce the elastic energy. We show that the diffraction profiles for thin

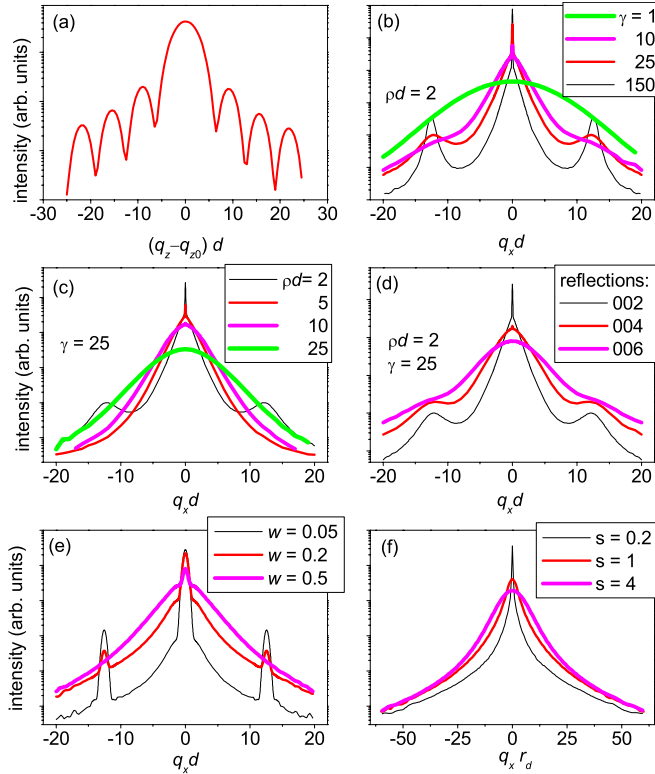


FIG. 1. (Color online) Peak profiles calculated by the Monte Carlo method for misfit (a–e) and threading (f) dislocations: (a) longitudinal scan and (b–d) transverse scans for misfit dislocations forming a Markov chain with the random increment chosen from the gamma distribution (the values of its parameter  $\gamma$  are indicated), (e) periodic misfit dislocations with random uncorrelated shifts (the shifts obey a Gaussian distribution with the standard deviation  $w$ ). Threading dislocations (f) are arranged in dipoles of random orientation and random width, the mean width is  $s$ .

films can be ascribed to the ordering of misfit dislocations. The experimental diffraction profiles for our GaN epitaxial films on SiC can be described only by simultaneously considering partially ordered misfit and threading dislocations. Misfit dislocations dominate in the diffraction peaks of thin films, while threading dislocations become important with increasing thickness. A fit of the experimental data with our model allows us to deduce the correlation of the dominant dislocation ensemble.

The Monte Carlo technique developed in this Brief Report is applicable to any type of dislocation distribution and any geometry of diffraction experiment. In the following, we describe it for the example of triple-crystal diffraction from an epitaxial film. Then, the scattering amplitude is  $A(q_x, q_z) = \int_{-\infty}^{\infty} dx \int_0^d dz e^{i[q_x x + q_z z + \mathbf{Q} \cdot \mathbf{U}(x, z)]}$ . Here  $\mathbf{Q}$  is the reciprocal lattice vector and  $\mathbf{q}$  is a deviation of the scattering vector from it,  $\mathbf{U}(x, z)$  is the displacement caused by elastic fields of all defects,  $x$  and  $y$  are the coordinates in the surface plane and  $z$  is along the surface normal. The film is limited by the surface  $z=0$  and the interface  $z=d$ . In writing a two-dimensional integral in the scattering plane  $xz$ , we assume integration of the scattered intensity over  $q_y$  by the vertical divergence of the beam in the diffractometer. This reciprocal-

space integration is equivalent to the projection on the plane  $y=0$  in the real-space integral.<sup>5</sup>

The scattered intensity is  $\mathcal{I}(q_x, q_z) = \langle |A(q_x, q_z)|^2 \rangle$ , where the angular brackets  $\langle \dots \rangle$  denote the average over the statistics of the dislocations. Both the spatial integration and the statistical average can be performed by the Monte Carlo method. However, a straightforward integration over  $x$  encounters a difficulty, since the integrand approaches a finite value in the limit  $x \rightarrow \infty$ , which results in a delta-function  $\delta(q_x)$  in the intensity. The experiment does not suffer from this difficulty because of the finite resolution. We therefore introduce a finite resolution in the Monte Carlo calculation to overcome this problem.

Let us consider a measurement of diffracted intensity  $\mathcal{I}(q_x, q_z)$  with a finite resolution  $\mathcal{R}(q_x)$ . We take into account the resolution in the  $x$  direction only. The resolution along  $q_z$  can be introduced in exactly the same way, but is not required as long as the resolution is sufficiently high to observe the thickness fringes. The finite-resolution intensity distribution is obtained as the convolution  $I(q_x, q_z) = \mathcal{I}(q_x, q_z) * \mathcal{R}(q_x)$ . We proceed from the convolution to the product of the Fourier transforms and represent the diffracted intensity as

$$I(q_x, q_z) = \int_{-\infty}^{\infty} dx \int \int_0^d dz_1 dz_2 \langle J \rangle R(x), \quad (1)$$

where

$$J = \exp\{i[q_x x + q_z(z_1 - z_2) + \mathbf{Q} \cdot \mathbf{U}(x, z_1) - \mathbf{Q} \cdot \mathbf{U}(0, z_2)]\}. \quad (2)$$

We require the resolution function  $R(x)$  to be normalized,  $\int_{-\infty}^{\infty} R(x) dx = 1$ , and rewrite the right-hand side of Eq. (1) as  $\int_{-\infty}^{\infty} F(x) R(x) dx$ . One can treat this latter integral as the function  $F(x)$  averaged over the probability density  $R(x)$ . Then, the Monte Carlo calculation of this integral consists in the summation of the values  $F(x)$  at the points  $x$  chosen according to the distribution  $R(x)$ .

The Monte Carlo estimate of the intensity Eq. (1) is the sum  $I(q_x, q_z) = VN^{-1} \sum_{n=1}^N J_n$ . Here  $N$  is the number of generated configurations, the  $n$ th configuration consisting of random coordinates  $x$ ,  $z_1$ ,  $z_2$  and a random set of dislocations, and  $J_n$  being the value of  $J$  calculated for this configuration by Eq. (2). The values of  $z_1$  and  $z_2$  are uniformly distributed from 0 to  $d$ . The values of  $x$  are chosen according to the resolution function  $R(x)$ . We take a Gaussian resolution function and use the random number generators readily available for the normal distribution. The dispersion  $\sigma_x$  of the Gaussian resolution function is the coherence length of the diffraction experiment. A “coherence volume”  $V$  is defined as  $V = \sqrt{2\pi} \sigma_x d^2$ . The dislocations are positioned according to the physical model of their correlations. This calculation is ideally suited for parallel implementation, since different parts of the sum can be calculated independently. The statistical error can also be estimated by the Monte Carlo method. It decreases as  $1/\sqrt{N}$  with the number  $N$  of generated configurations, exactly as the photon counting statistics in the experiment.

As a first example, we consider correlated misfit disloca-

tions. The dislocation positions  $x_j$  at the interface  $z=d$  are generated as a stationary Markov chain: once the position of a dislocation  $x_j$  is specified, the position of the next dislocation is  $x_{j+1}=x_j+\delta x$ , where the random increment  $\delta x$  does not depend on  $j$ . Its mean is the average distance between dislocations,  $\langle\delta x\rangle=\rho^{-1}$ , where  $\rho$  is the linear dislocation density. We pick the random increments  $\delta x$  from the gamma distribution and vary its parameter  $\gamma$ . The displacements are calculated, in linear elasticity, as a sum of the contributions of the individual dislocations,  $\mathbf{U}(x,z)=\sum_j\mathbf{u}(x-x_j,z)$ , where  $\mathbf{u}(x,z)$  is the displacement due to a dislocation located at  $(0,d)$ . Explicit expressions for the displacements due to a dislocation parallel to the free surface are well known.<sup>5</sup>

Figures 1(a)–1(d) show the calculated peak profiles for this model. The longitudinal scan ( $q_z$  scan) in Fig. 1(a) reveals the thickness fringes. The peak position is determined by the mean displacement,  $\langle\mathbf{Q}\cdot\mathbf{U}(x,z)\rangle=q_{z0}z$ . Here  $q_{z0}=[\nu/(1-\nu)]\rho Q_z b_x$ , where  $b_x$  is the  $x$  component of the Burgers vector and  $\nu$  is the Poisson ratio. This mean value is calculated analytically<sup>5</sup> and verified here by means of the Monte Carlo calculation. All transverse scans ( $q_x$  scans) below are performed at the maximum of the longitudinal scan,  $q_z=q_{z0}$ . Figure 1(b) presents the transformation of the peak profile with the increasing order of the dislocations by varying the parameter  $\gamma$  of the gamma distribution. Uncorrelated dislocations ( $\gamma=1$ , thick line) give rise to a broad Gaussian peak.<sup>5</sup> Correlated dislocations ( $\gamma>1$ ) result in a narrowing of the diffuse peak and the appearance of a central coherent peak. Satellite peaks of finite width appear for  $\gamma\gg 1$  and become narrower as  $\gamma$  is increased. The positions of the satellites correspond to the mean distance between dislocations,  $q_x=2\pi\rho m$ , where  $m$  is an integer. Very similar diffraction patterns with broadened satellite reflections were observed experimentally for GaSb/GaAs(001) films.<sup>13,14</sup> Figs. 1(c) and 1(d) show that the increase in either misfit, or film thickness or the reflection order reduces the coherent peak. The diffuse peaks are broader in the higher-order reflections, Fig. 1(d). However, the angular width of the peak proportional to  $q_x/n$  remains the same with the increasing reflection order  $n$ , in an agreement with the experiment.<sup>11,12</sup>

The shape of the diffuse peak around the central coherent peak is close to an exponential (straight line in logarithmic scale). This shape is characteristic for many other experiments,<sup>7–12,15–17</sup> but a closer inspection shows that some of the observed slopes are notably smaller than the ones in Fig. 1(b)–1(d). We therefore explore correlations of another type in Fig. 1(e). The dislocation positions are now obtained by equidistant placement of the dislocations,  $x_j=j\rho^{-1}$ , and the addition of uncorrelated random shifts  $\delta x$  with zero mean ( $\langle\delta x\rangle=0$ ). The particular distribution of the shifts does not play a role, but the width of the distribution does. Figure 1(e) presents the results for the Gaussian distribution of shifts with different standard deviations  $w$ . Both the central peak and the satellites are resolution limited. The intensity of the satellites decreases as  $w$  is increased. The satellites vanish when the random shifts become comparable with the mean distance between dislocations (thick curve).

The same Monte Carlo method can be applied to study threading dislocations going through the film along the surface normal. We restrict the analysis to the symmetric Bragg

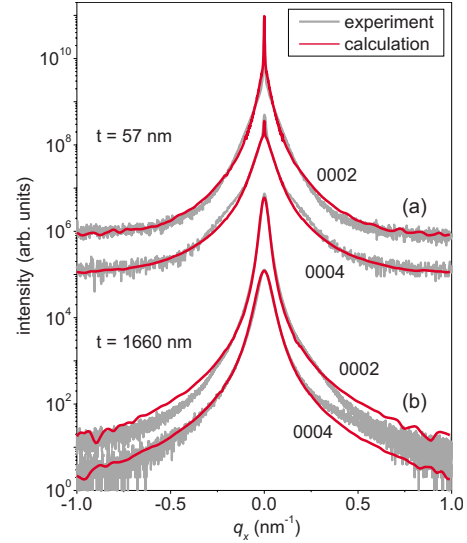


FIG. 2. (Color online) Symmetric Bragg peaks from (a) 57 nm and (b) 1660-nm-thick GaN epitaxial films on 6H-SiC. Experimental (thick gray curves) and calculated (thin curves) peak profiles are compared.

reflection, which is sensitive to screw dislocations. We have already found that the strain fields of threading dislocations in epitaxial films are screened by surrounding dislocations,<sup>2</sup> and our aim now is to propose and evaluate a physical model of this screening. We generate screw threading dislocations as positionally uncorrelated dislocation dipoles of random width. The widths are taken from an exponential distribution with the mean value  $s$ , which may be smaller or larger than the mean distance between dislocations  $r_d$ . Figure 1(f) presents the calculated peaks. When  $s$  is much smaller than the mean distance between dislocations, the dislocation ensemble consists of the dipoles and a sharp diffraction peak appears [thin black line in Fig. 1(f)]. In the opposite limit  $s\gg r_d$ , the dislocations are almost uncorrelated and the central part of the peak is a broad Gaussian (thick line). The curves have a common  $q^{-3}$  asymptotic.<sup>2</sup> All curves in Fig. 1(f) are calculated for the same dislocation density. This plot shows that the peak width can strongly vary depending on the correlations between dislocations.

We apply the Monte Carlo method outlined above to study the x-ray diffraction profiles from two GaN films grown on 6H-SiC(0001) by molecular beam epitaxy. Details of the growth conditions and the morphology of these films can be found in Ref. 2. The thin (57 nm) sample in the present work has been fabricated under the same conditions as sample 1 in this previous work, whereas the thick (1660 nm) sample is identical to sample 2. For the thin sample, we used Ga rich growth conditions which promote a rapid smoothing of the growth front and minimize the density of screw dislocations. In contrast, the near-stoichiometric conditions employed for the thick sample result in a lower density of edge dislocations. The symmetric  $\omega$  scans were measured on a Philips XPert diffractometer in a triple-axis configuration with a three-bounce Ge(022) analyzer.

The diffraction peaks of the thin sample, Fig. 2(a), are quite similar to these reported for a wide variety of epitaxial

systems.<sup>7–12,15–17</sup> The diffraction peaks consist of a sharp central peak and the exponentially decaying diffuse scattering. The central peak is less intense in the second-order reflection. A closer inspection of the central peak shows that its angular width of  $36''$  is about four times larger than the instrumental resolution. We attribute the peak broadening to threading dislocations. Hence, we perform Monte Carlo calculation taking into account both misfit and threading dislocations with the respective correlations. The GaN/SiC misfit of 3.3% is released by three (due to the hexagonal symmetry of the interface) arrays of dislocations. The dislocation density in each array is then  $\rho d \approx 4$ . In the Monte Carlo calculation, the three arrays are generated independently by dislocations that are randomly shifted from periodic positions. The standard deviation in the shifts  $w$  obtained from the fit to the experimental curve is 0.35 of the mean distance between dislocations. The observed central peak broadening is not sufficient to obtain both the density of threading dislocations and their correlations. We use the screw threading dislocation density of  $10^8 \text{ cm}^{-2}$ , as estimated from the observed density of surface pits in atomic force microscopy, and obtain a mean width of the dislocation dipoles of  $0.4r_d$  from the comparison of the experimental and calculated profiles. The calculated peaks in Fig. 2(a) demonstrate the possibility to simultaneously simulate the misfit and threading dislocations and to obtain characteristic correlations for both of them.

When the film thickness is increased, the diffraction intensity due to the same ensemble of threading dislocations would increase, with the shapes of the peaks remaining the same. Quite surprisingly, however, the diffraction peaks of

the thick GaN sample, Fig. 2(b), are much broader than the central peak of the thin sample. Assuming that the peaks in Fig. 2(b) are due to screw threading dislocations only, we can determine both their density and the correlations. A separate calculation confirms that the contribution of misfit dislocations is indeed small. The calculated profiles in Fig. 2(b) are obtained for a threading dislocation density of  $1 \times 10^9 \text{ cm}^{-2}$  and dislocation dipoles with a mean width  $s$  two times larger than the mean distance between dislocations. The dislocation density is in a good agreement with the one obtained in Ref. 2 from the double-crystal diffraction curves. Hence, compared to the thin sample, the dislocation density is larger by an order of magnitude, and the correlations between dislocations are notably weaker.

The sharp central peak is commonly observed in our thin GaN samples. Its presence indicates that the displacement fields of screw threading dislocations are strongly screened, e.g., by formation of the dipoles. The broad peaks from the thick samples indicate much weaker correlations. Therefore, threading dislocations do not simply propagate through the film but decorrelate as the film grows.

In summary, the Monte Carlo method presented here allows a straightforward calculation of the diffraction profiles for arbitrary dislocation arrays, any type of correlations, and any diffraction geometry. With its help, we explain the lineshape universally reported for thin epitaxial films.<sup>6–17</sup> As in the case of our own experimental results from GaN films on SiC, this lineshape is caused by correlated distributions of misfit dislocations.

<sup>1</sup>M. Wilkens, *Krist. Tech.* **11**, 1159 (1976).

<sup>2</sup>V. M. Kaganer, O. Brandt, A. Trampert, and K. H. Ploog, *Phys. Rev. B* **72**, 045423 (2005).

<sup>3</sup>S. Daniš, V. Holý, Z. Zhong, G. Bauer, and O. Ambacher, *Appl. Phys. Lett.* **85**, 3065 (2004).

<sup>4</sup>S. Daniš and V. Holý, *J. Alloys Compd.* **401**, 217 (2005).

<sup>5</sup>V. M. Kaganer, R. Köhler, M. Schmidbauer, R. Opitz, and B. Jenichen, *Phys. Rev. B* **55**, 1793 (1997).

<sup>6</sup>P. M. Reimer, H. Zabel, C. P. Flynn, and J. A. Dura, *Phys. Rev. B* **45**, 11426 (1992).

<sup>7</sup>A. Gibaud, R. A. Cowley, D. F. McMorrow, R. C. C. Ward, and M. R. Wells, *Phys. Rev. B* **48**, 14463 (1993).

<sup>8</sup>A. Gibaud, D. F. McMorrow, and P. P. Swaddling, *J. Phys.: Condens. Matter* **7**, 2645 (1995).

<sup>9</sup>M. Huth and C. P. Flynn, *Appl. Phys. Lett.* **71**, 2466 (1997).

<sup>10</sup>A. R. Wildes, R. A. Cowley, R. C. C. Ward, M. R. Wells, C. Jansen, L. Wiren, and J. P. Hill, *J. Phys.: Condens. Matter* **10**, L631 (1998).

<sup>11</sup>P. F. Miceli and C. J. Palmstrøm, *Phys. Rev. B* **51**, 5506 (1995).

<sup>12</sup>P. F. Miceli, J. Weatherwax, T. Krentsel, and C. J. Palmstrøm, *Physica B* **221**, 230 (1996).

<sup>13</sup>A. Yu. Babkevich, R. A. Cowley, N. J. Mason, and A. Stunault, *J. Phys.: Condens. Matter* **12**, 4747 (2000).

<sup>14</sup>A. Yu. Babkevich, R. A. Cowley, N. J. Mason, S. Weller, and A. Stunault, *J. Phys.: Condens. Matter* **14**, 13505 (2002).

<sup>15</sup>M. Becht, F. Wang, J. G. Wen, and T. Morishita, *J. Cryst. Growth* **170**, 799 (1997).

<sup>16</sup>A. Boule, R. Guinebrière, and A. Dager, *J. Appl. Phys.* **97**, 073503 (2005).

<sup>17</sup>S. Gariglio, N. Stucki, J.-M. Triscone, and G. Triscone, *Appl. Phys. Lett.* **90**, 202905 (2007).

<sup>18</sup>R. I. Barabash, W. Donner, and H. Dosch, *Appl. Phys. Lett.* **78**, 443 (2001).

<sup>19</sup>M. A. Krivoglaz, *X-Ray and Neutron Diffraction in Nonideal Crystals* (Springer, Berlin, 1996).

<sup>20</sup>V. Holý, T. Baumbach, D. Lübbert, L. Helfen, M. Ellyan, P. Mikulík, S. Keller, S. P. DenBaars, and J. Speck, *Phys. Rev. B* **77**, 094102 (2008).